Plenary lecture, 13th International Conference on Flow Dynamics
October 10-12, 2016, Sendai, Japan

Energy conversion in transient molecular plasmas:

Implications for plasma flow control and plasma assisted combustion

Igor Adamovich

Department of Mechanical and Aerospace Engineering
Ohio State University

OSU NETLab

Faculty: Igor Adamovich, Walter Lempert, and J. William Rich

Research backgrounds of students and post-docs: Mechanical Engineering, Aerospace Engineering, Electrical Engineering, Chemical Physics, Physical Chemistry, Physics

Outline

I. Motivation: critical importance of energy transfer processes in nonequilibrium, high-pressure molecular plasmas

II. Electric field: discharge energy loading and partition

III. Electron density and electron temperature: discharge energy loading and partition

IV. Dynamics of temperature rise: “rapid” heating and “slow” heating

V. Air and fuel-air plasma chemistry: kinetics of plasma assisted combustion

VI. Air plasma kinetics and plasma flow control

VII. Summary and future outlook

I. Motivation

Energy Partition in Air Plasma vs. Electric Field

Yu. Raizer, Gas Discharge Physics, Springer, 1991

(1) O_2 vibrational excitation:
Non-self-sustained discharges,
very low E/N

(4) N_2 vibrational excitation:
Quasi-steady-state discharges,
low E/N

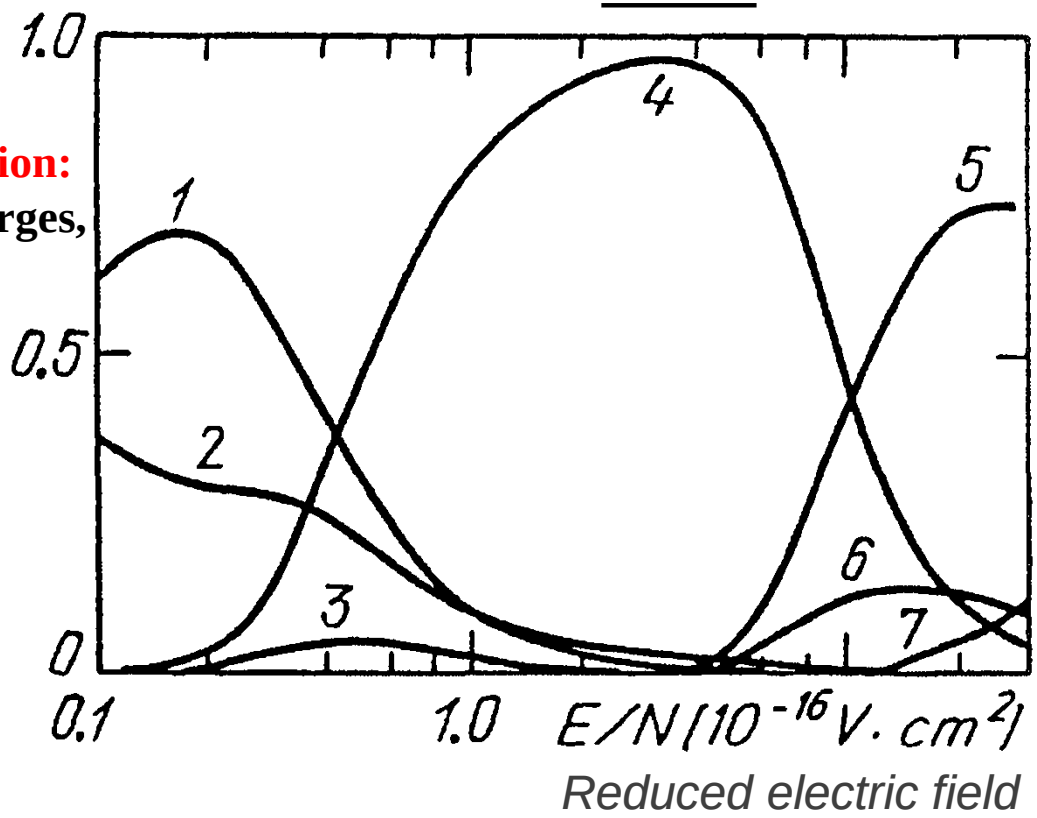

(5,6) electronic excitation, dissociation, (7) ionization:
Pulsed discharges, high E/N

- **Reduced electric field, E/N, controls input energy partition in the discharge**
- **Rates of electron impact processes: strongly (exponentially) dependent on E/N**

Energy conversion in molecular plasmas: here is what we know

- **Energy is coupled to electrons and ions by applied electric field**
- **Electric field in the plasma: controlled by electron and ion transport, and by surface charge accumulation**
- **Energy partition (vibrational and electronic excitation, dissociation, ionization): controlled by electron density and electric field (or electron temperature)**
- **Temperature rise in discharge afterglow: controlled by quenching of excited electronic states, vibrational relaxation**
- **Plasma chemical reactions, rates of radical species generation: controlled by populations of excited electronic states, e.g. N_2*, excited vibrational states, e.g. $N_2(v)$**
- **Time-resolved measurements of $\vec{E}$, n_e, T_e, N_2^*, $N_2(v)$, and radical species *(O, H, OH, NO, CH, HO_2, CH_2O)*: stable, reproducible, high-pressure ns pulse discharges**
- **Objective: quantitative insight into energy conversion mechanisms critical for plasma-assisted combustion and plasma flow control**

THE OHIO STATE UNIVERSITY

II. Electric field in transient plasmas: insight into discharge energy loading and partition

Diagnostics: CARS-like 4-wave mixing

2-D Ns Pulse Discharge in Atmospheric Air

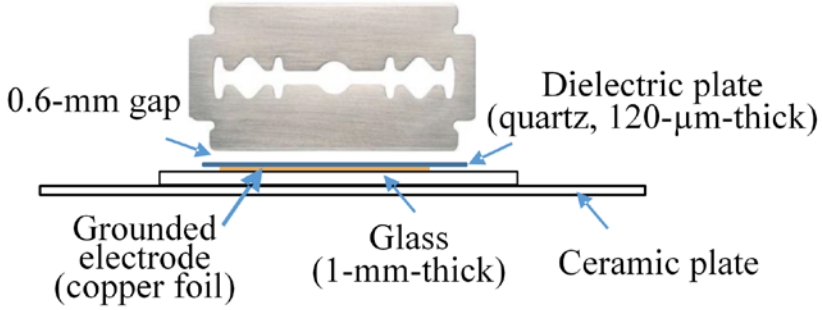

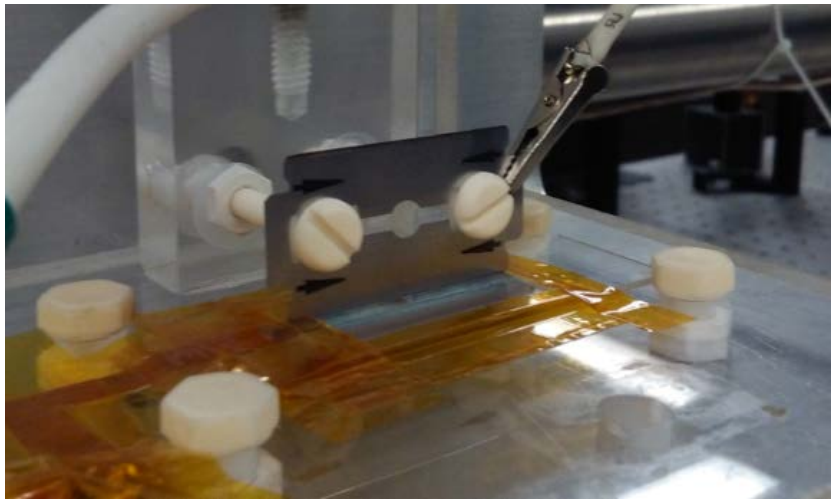

- **Discharge sustained between a high-voltage electrode (razor blade) and grounded copper foil, covered with quartz plate 120 μm thick**
- **Discharge gap 600 μm**
- **Simple two-dimensional geometry, diffuse plasma**

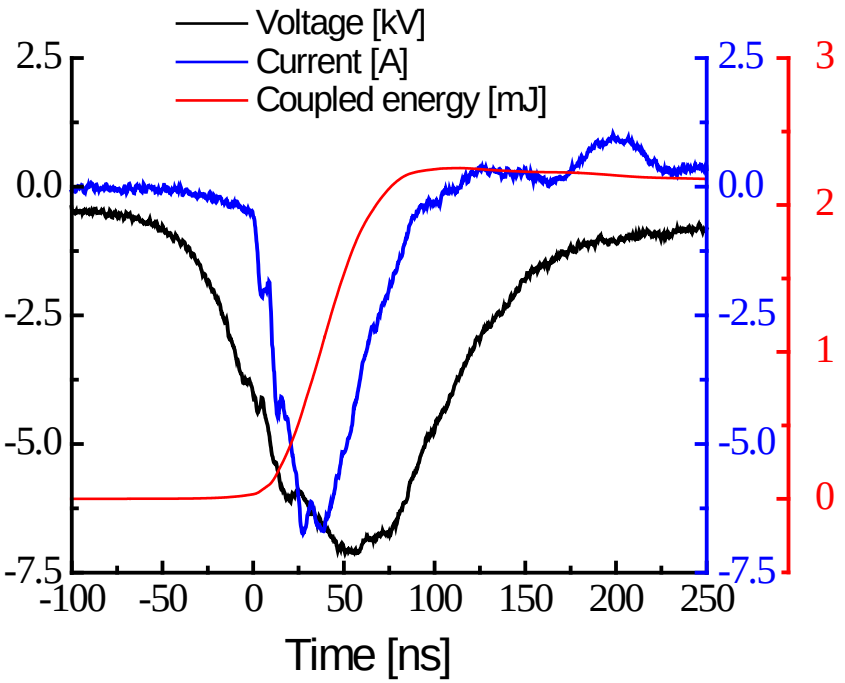

- **Peak voltage 7.5 kV, peak current 7 A, coupled energy 2 mJ**
- **Two current peaks of opposite polarity: “forward” and “reverse” breakdowns**
- **Time-resolved electric field measured at several locations in the plane of symmetry**
- **Electric field distribution along the surface is also measured**

“Curtain Plasma” Images, Negative Polarity Pulse

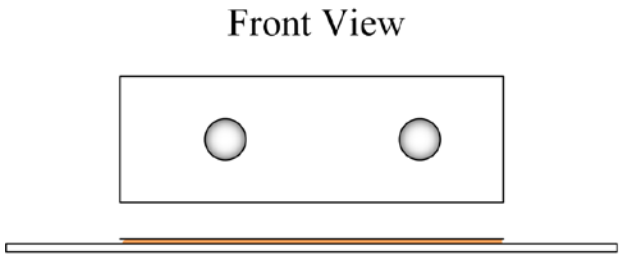

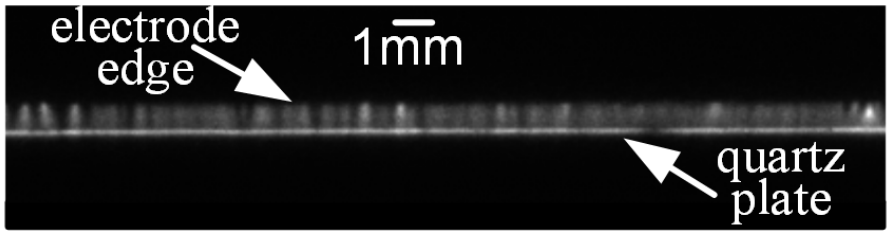

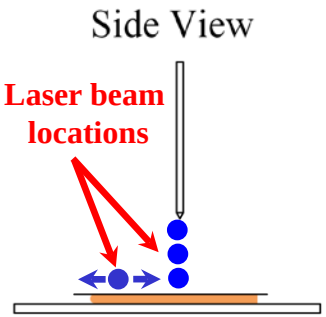

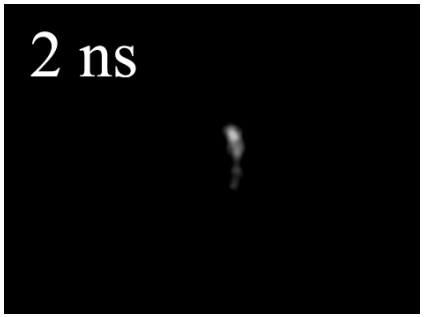

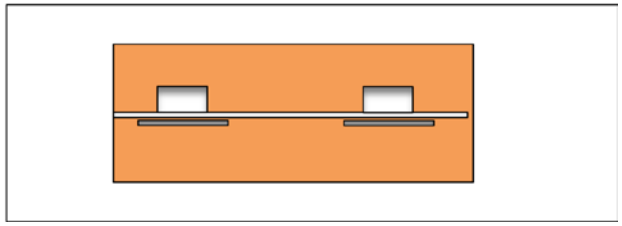

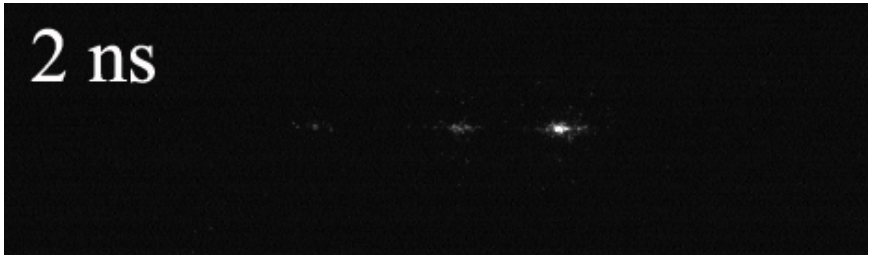

- Front view: near-diffuse plasma “curtain”
- Diffuse surface ionization wave detected, straight ionization front
- Wave speed ~ 0.03 mm/ns
- Surface plasma layer thickness ~150 μm

Time-resolved and Spatially-Resolved Electric Field Measurements

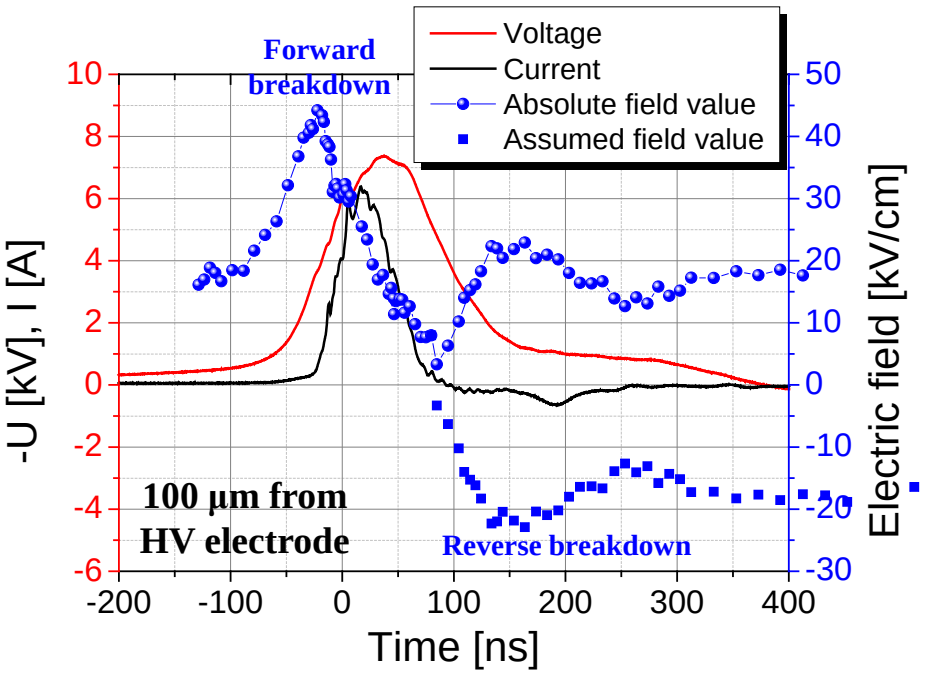

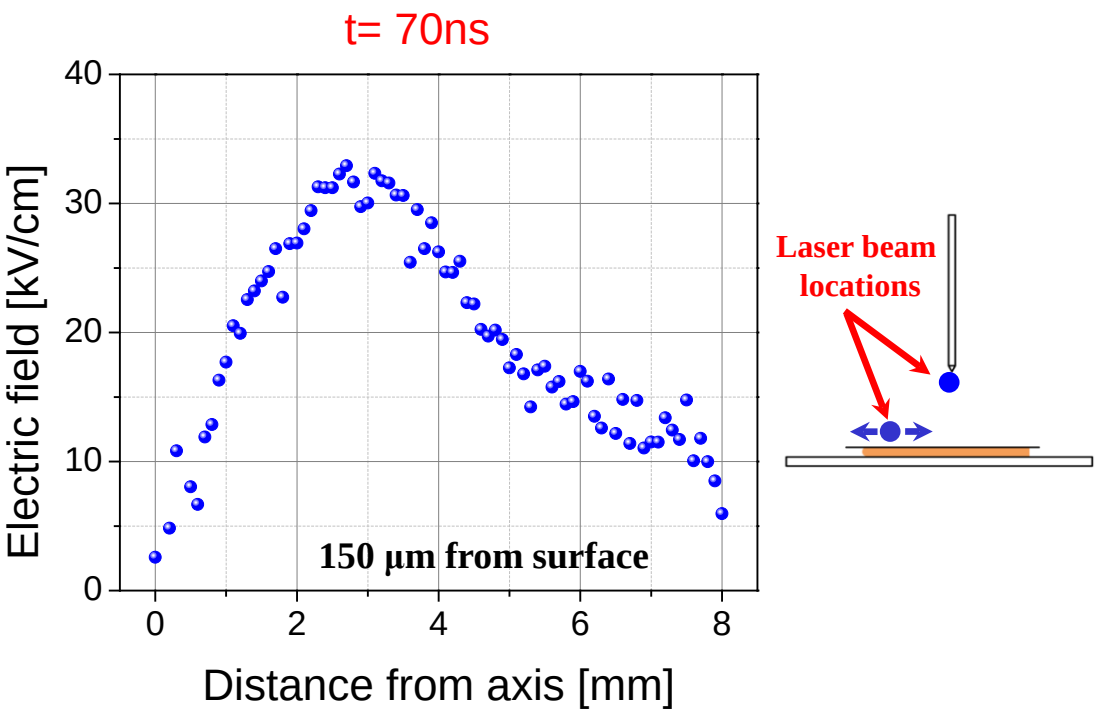

- **Initial field offset: charge accumulation on dielectric surface from previous pulse**
- **Field follows applied voltage rise, increases until "forward breakdown"**
- **After breakdown, field reduced due to charge accumulation on dielectric surface**
- **Field is reversed after applied voltage starts decreasing**
- **After discharge pulse, field decays over several µs: surface charge neutralization by charges from plasma**

- **Field distribution measured at the moment when field reversal occurs near HV electrode (t=70 ns)**
- **"Snapshot" electric field distribution across the surface ionization wave front**

III. Electron density and electron temperature in transient plasmas: insight into discharge energy loading and partition

Diagnostics: Thomson scattering

Filtered Thomson Scattering: n_e , T_e, and EEDF inference

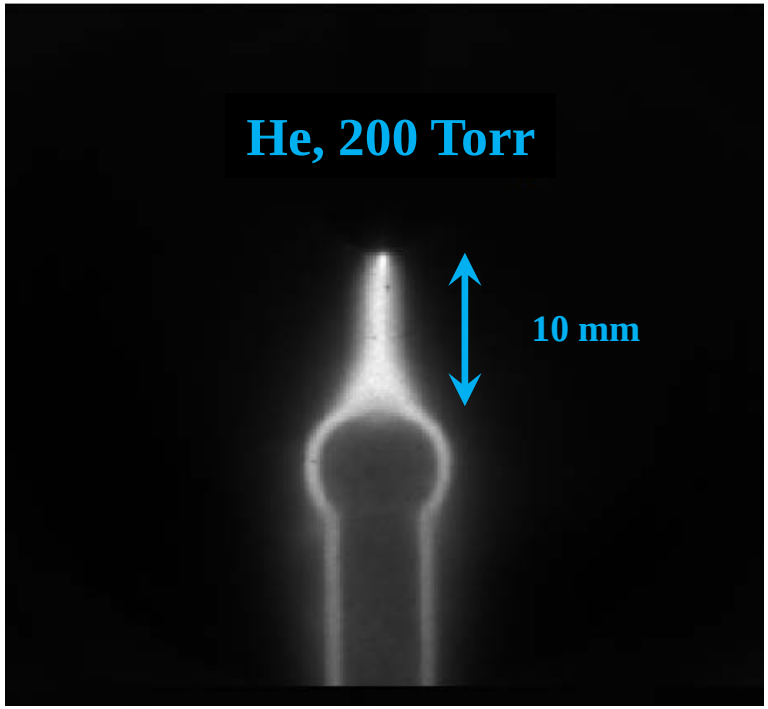

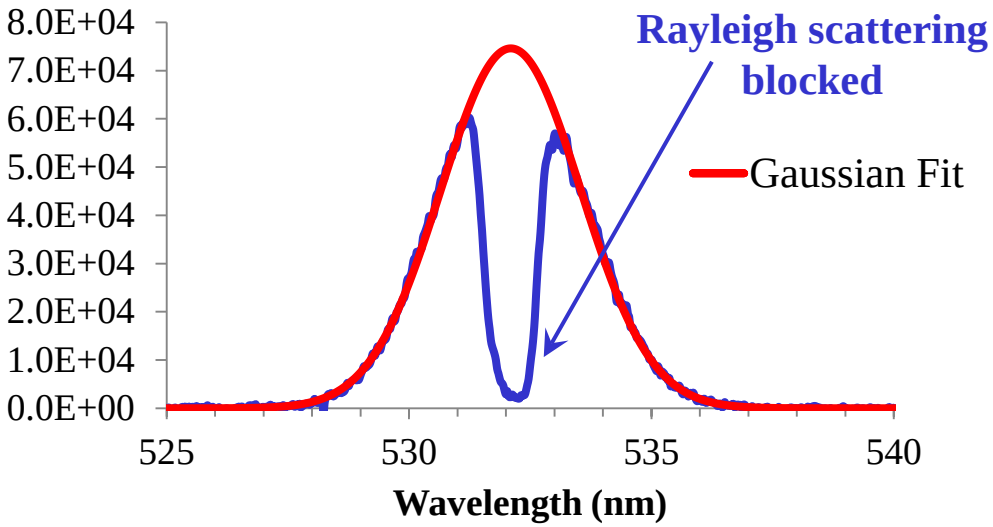

- **Electron density: area under Thomson scattering spectrum**
- **Electron temperature: spectral linewidth**
- **Raman scattering rotational transitions in N_2 used for absolute calibration**
- **Gaussian Thomson scattering lineshape: Maxwellian EEDF**

N_2 Raman scattering

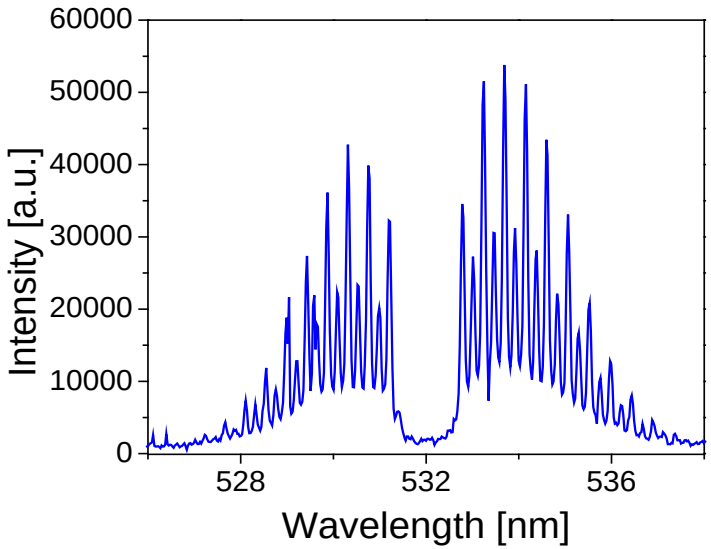

Thomson Scattering Spectra

Sphere-to-sphere ns pulse discharge in H_2-He and O_2-He

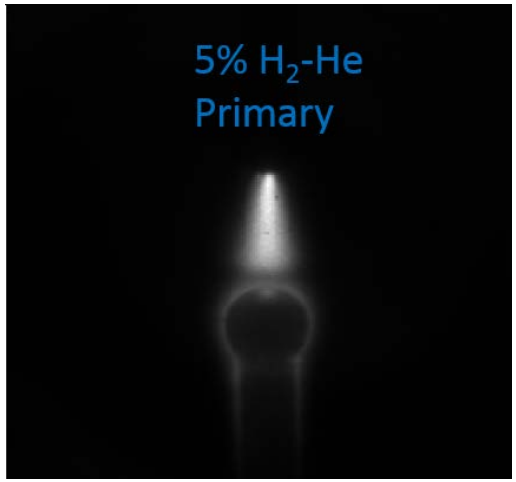

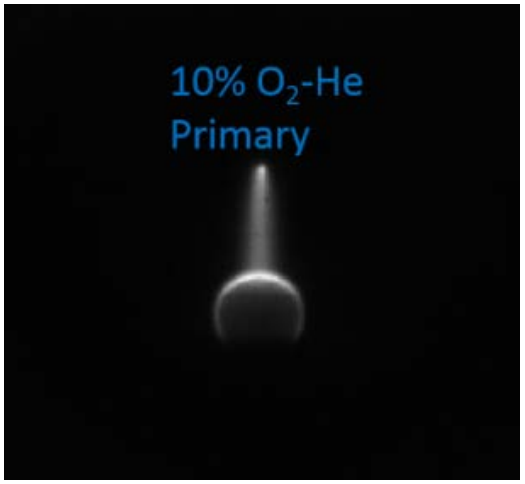

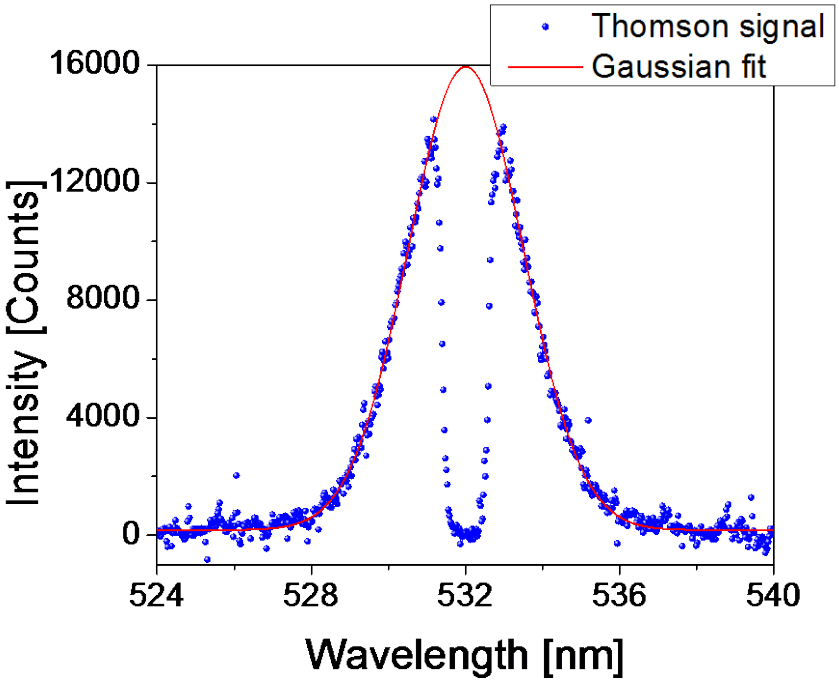

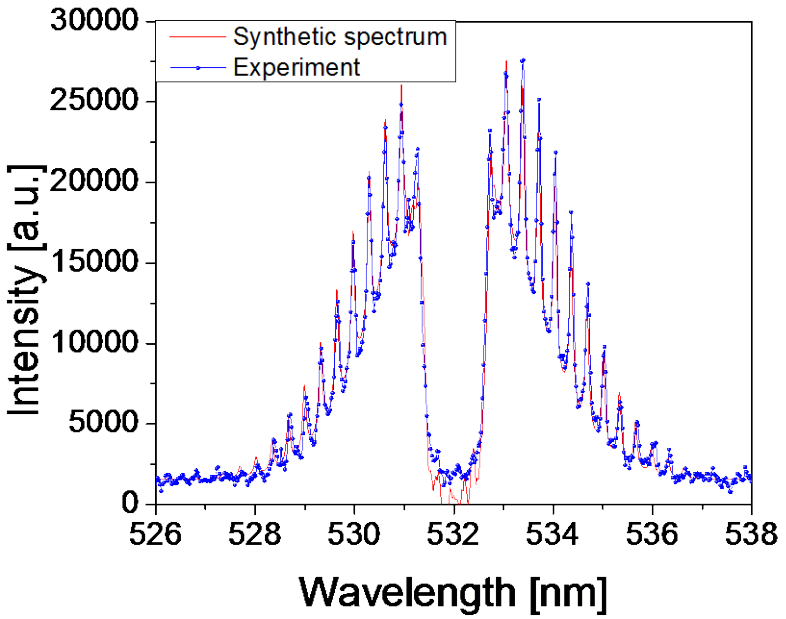

5% H_2-He, P=100 torr, t=100 ns

$n_e = 1.5 \cdot 10^{14}$ cm^{-3}, T_e = 2.0 eV

10% O_2-He, P=100 torr, t=100 ns

$n_e = 1.7 \cdot 10^{13}$ cm^{-3}, T_e= 1.6 eV, T=350 K

Electron Density and Electron Temperature

Sphere-to-sphere ns pulse discharge in O_2-He

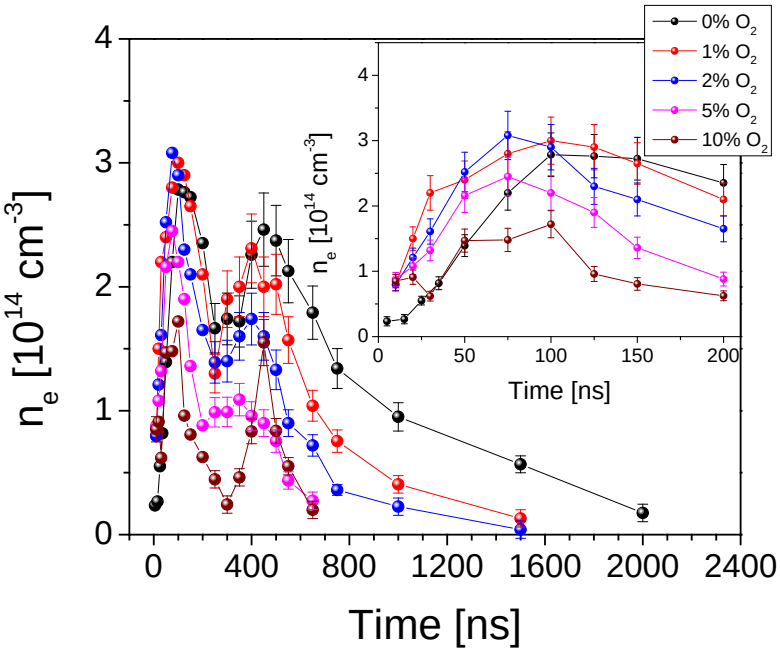

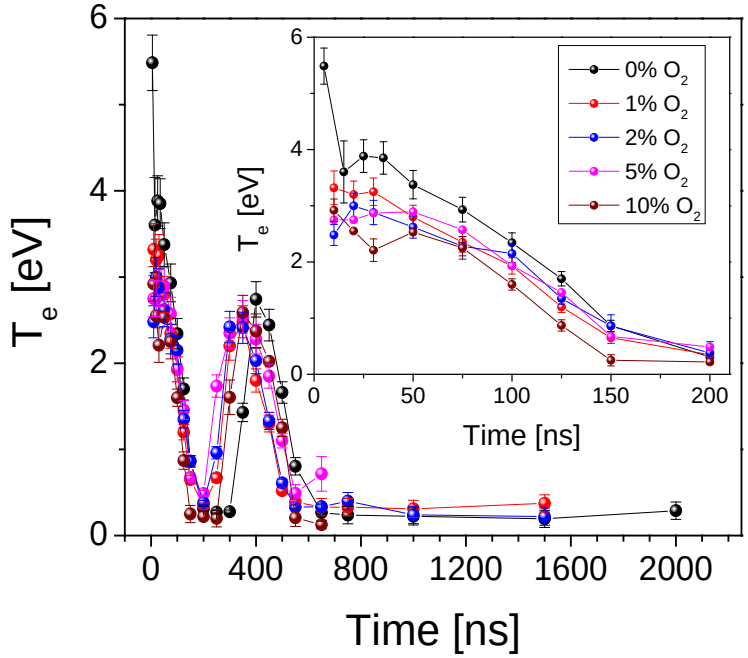

- $n_e = 10^{13}$ - $3 \cdot 10^{14}$ cm^{-3} , $T_e = 0.3 – 5.5$ eV (0-10% O_2)
- "Double maxima" in n_e, T_e : two discharge pulses ≈400 ns apart
- Electron temperature in the afterglow $T_e \approx 0.3$ eV
  Superelastic collisions prevent electron cooling
- Modeling predictions in good agreement with data

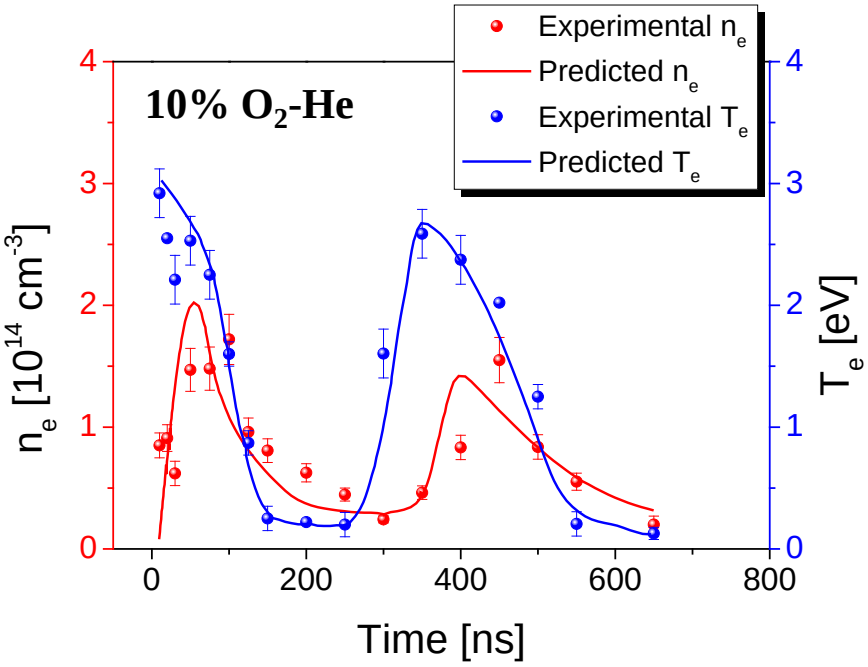

IV. Dynamics of temperature rise in transient plasmas: "rapid" heating and "slow" heating

Diagnostics: vibrational and pure rotational ps CARS

Sphere-to-sphere ns pulse discharge in air, P=100 Torr
Discharge pulse waveforms and CARS spectra

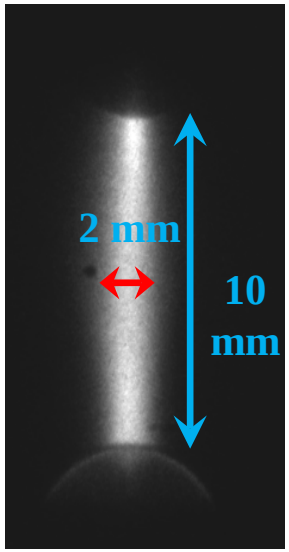

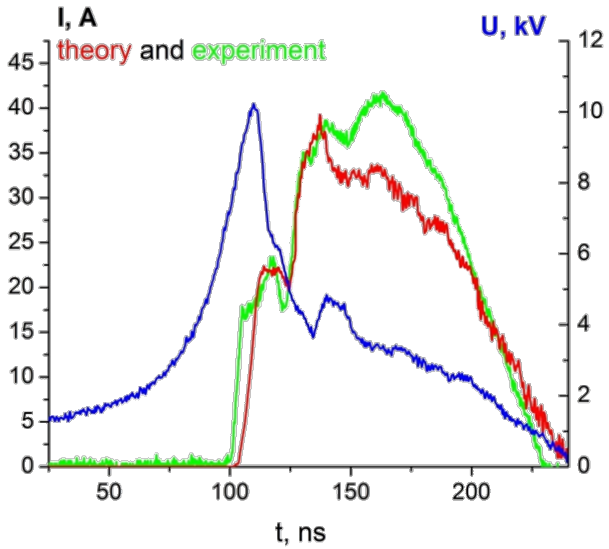

Pulse energy coupled to plasma ~ 0.5 eV

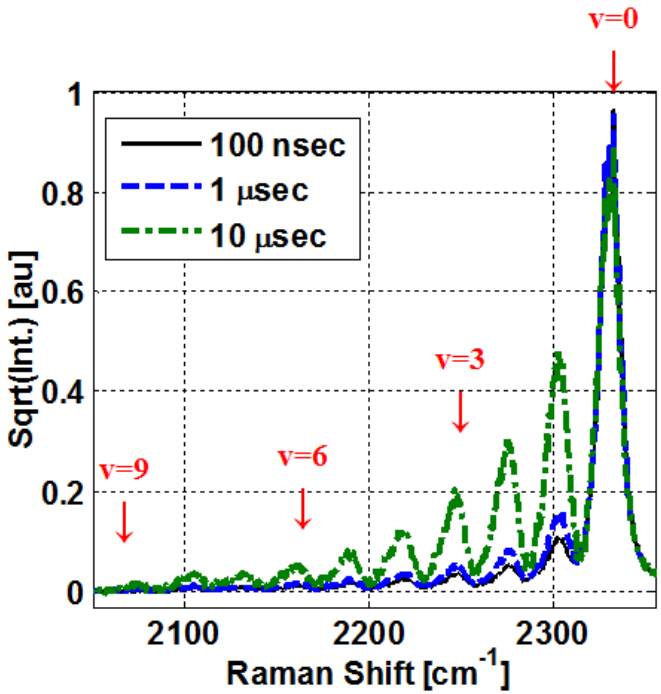

N_2(v=0-9) bands during and after discharge pulse

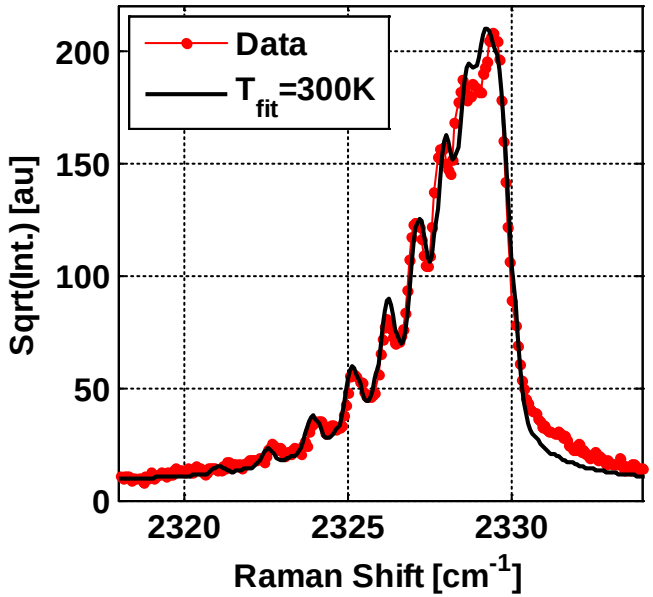

N_2(v=0) band (without plasma)

Temperature rise in ns pulse discharge and afterglow: air vs. nitrogen

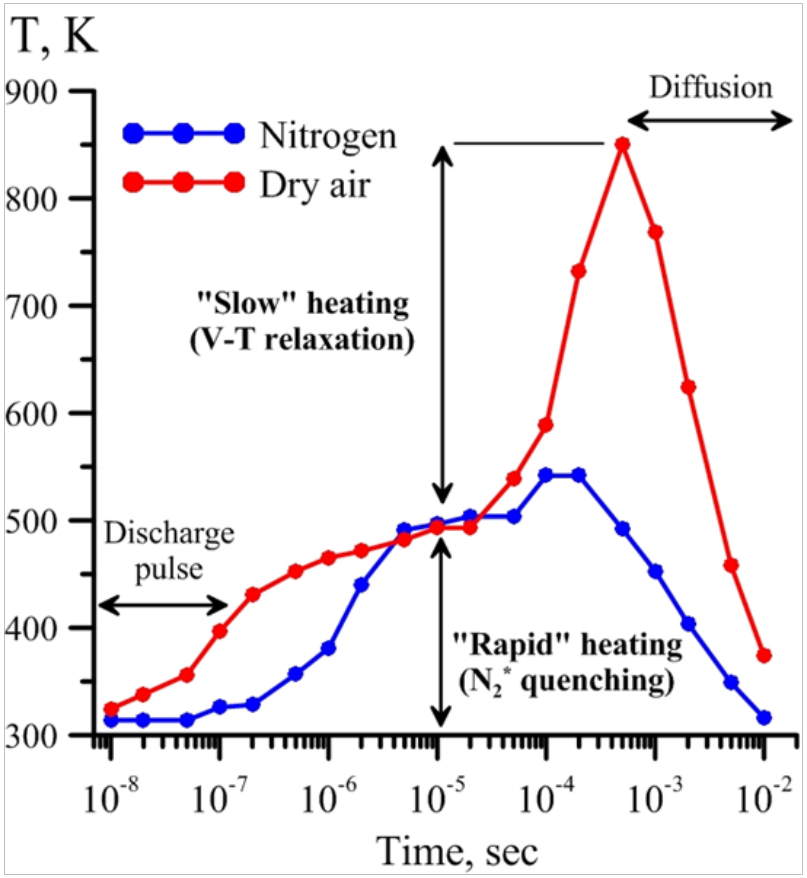

Air, P=100 Torr

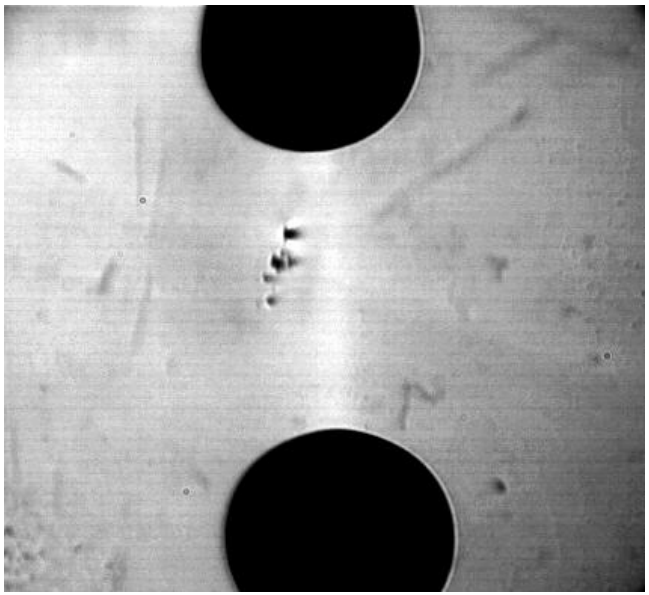

t= 1-10 μs (frames are 1 μs apart)

- **Compression waves formed by "rapid" heating, on sub-acoustic time scale, $\tau_{acoustic} \sim r / a \sim 2$ μs**
- **Strong effect on high-speed flows**

Comparison with modeling predictions in air: vibrational kinetics and temperature rise

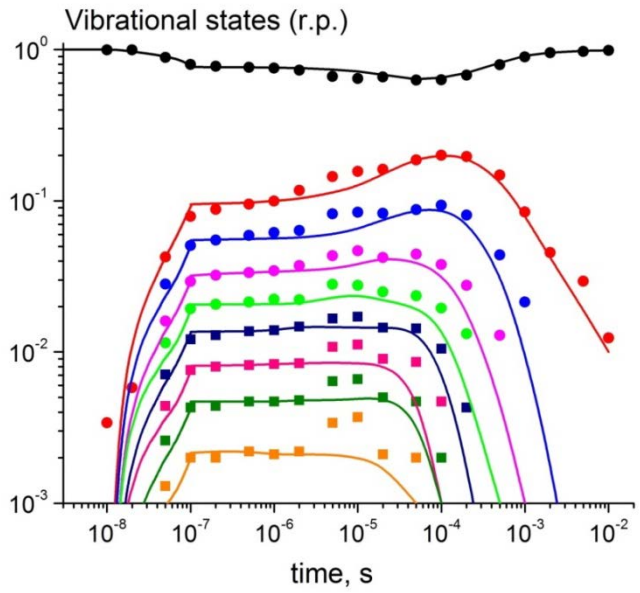

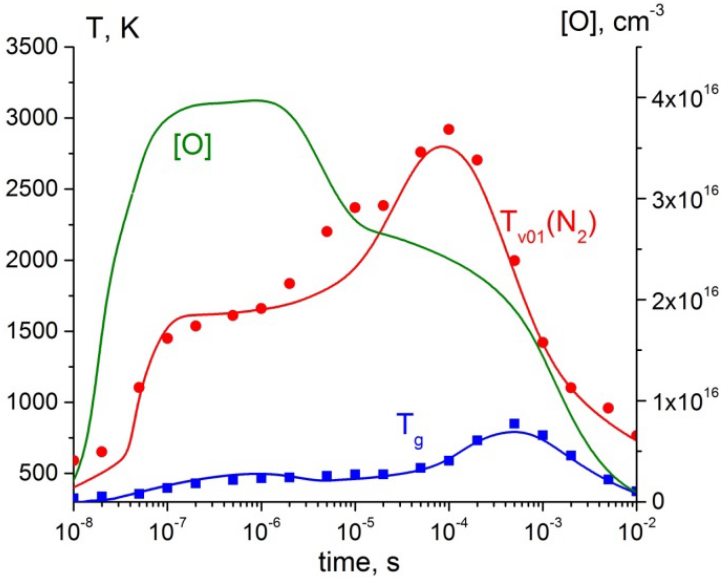

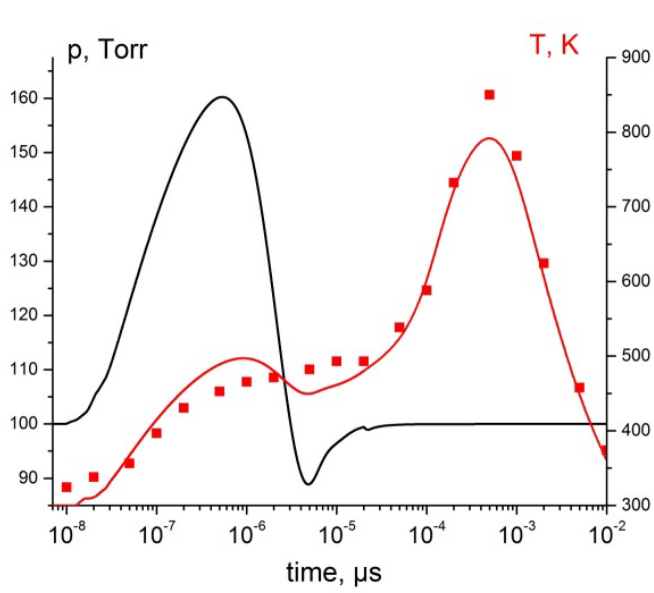

- Strong vibrational excitation in the discharge, $N_2(v=0\text{-}8)$
- $T_v(N_2)$ rise in early afterglow: V-V exchange, $N_2(v) + N_2(v=0) \rightarrow N_2(v\text{-}1) + N_2(v=1)$
- $T_v(N_2)$ decay in late afterglow: V-T relaxation, $N_2(v) + O \rightarrow N_2(v\text{-}1) + O$, radial diffusion
- "Rapid" heating: quenching of N_2 electronic states, $N_2(C,B,A,a) + O_2 \rightarrow N_2(X) + O + O$
- "Slow" heating: V-T relaxation, $N_2(X,v) + O \rightarrow N_2(X,v\text{-}1) + O$
- "Rapid" heating: pressure overshoot on centerline, compression waves detected in experiments
- NO formation: dominated by reactions of N_2 electronic states, $N_2^* + O \rightarrow NO + N$, also in good agreement with [NO], [N] measurements

Adding CO_2 (rapid V-T relaxer) to air: accelerating energy thermalization rate

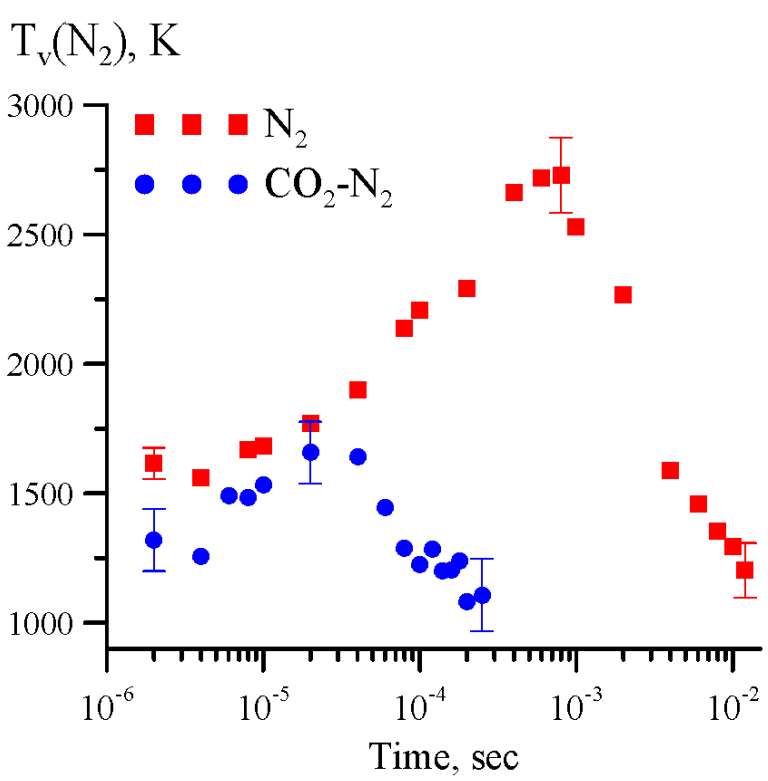

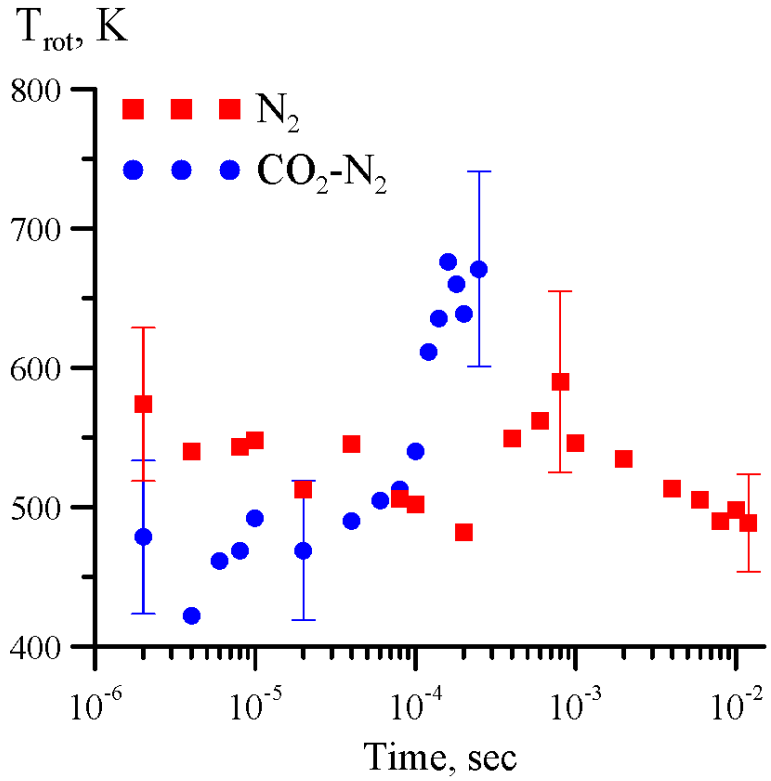

Rapid N_2 relaxation and temperature rise. Mechanism of accelerated heating:

- **V-V energy exchange between N_2 and $CO_2(\nu_3)$ mode: $N_2(v=1) + CO_2(000) \leftrightarrow N_2(v=0) + CO_2(001)$**
- **CO_2 energy re-distribution among vibrational modes: $CO_2(001) + M \leftrightarrow CO_2(100,020,010) + M$**
- **V-T relaxation of bending mode: $CO_2(010) + M \rightarrow CO_2(100) + M$**
- **Strong effect on nonequilibrium compressible flows**

V. Fuel-air chemistry in transient plasmas: kinetics of plasma assisted combustion

Diagnostics: Rayleigh scattering, LIF, CARS

Plasma chemical reactions and transport: ns pulse discharge in H_2 - O_2 - Ar, P=40 torr

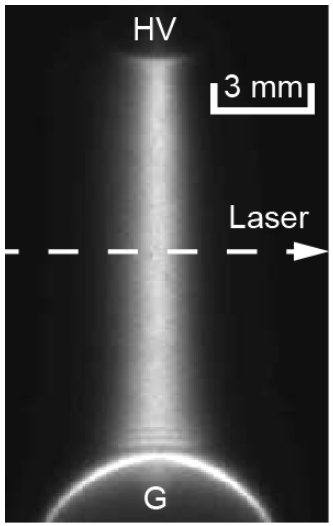

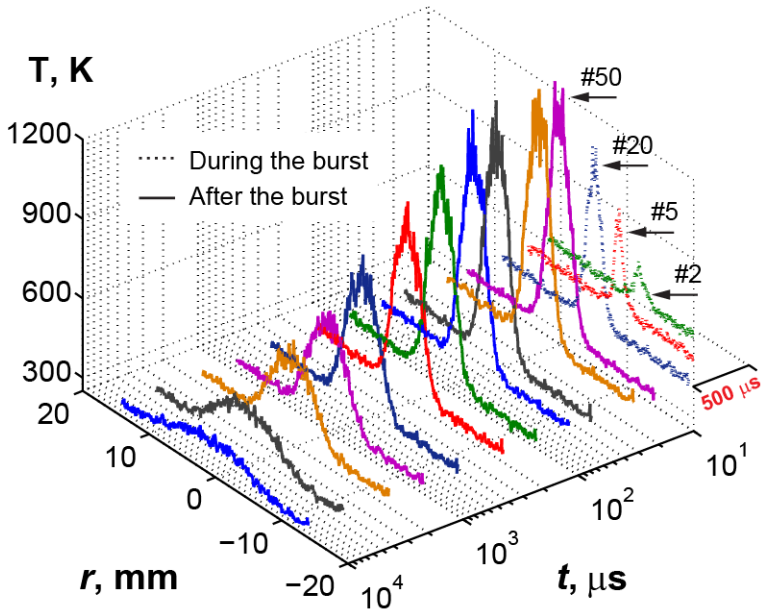

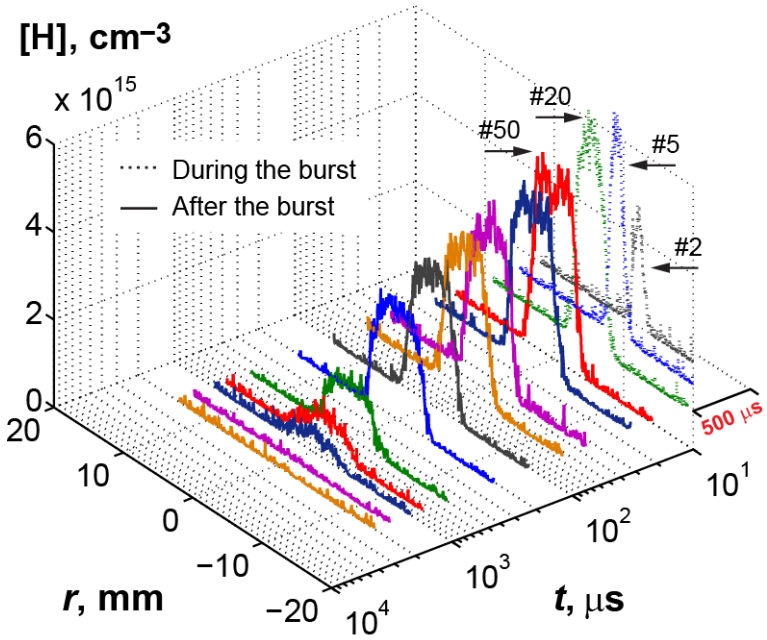

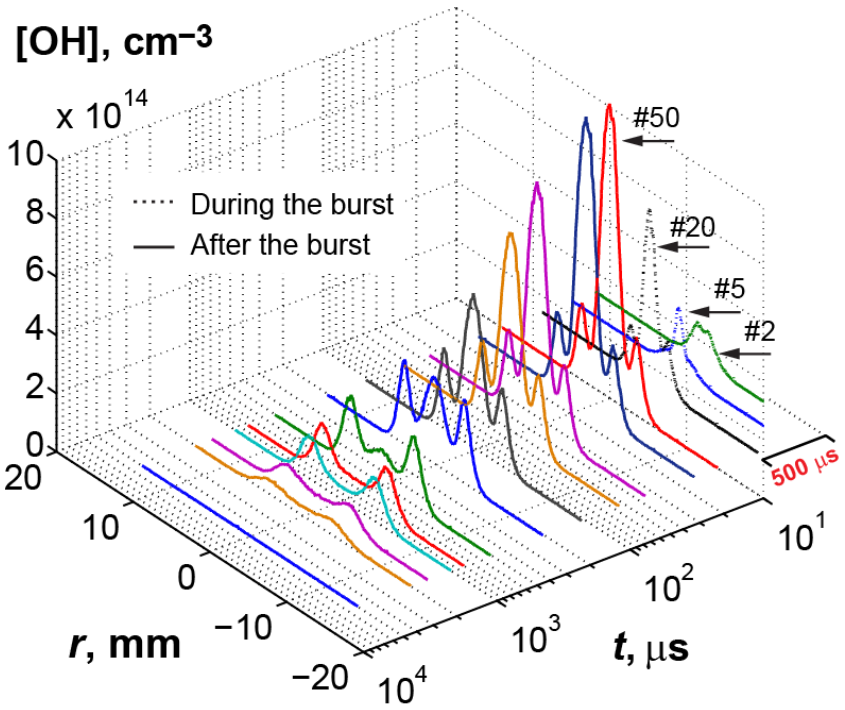

Hot central region:

OH production dominated by chain branching

$$H + O_2 \rightarrow OH + O \quad ; \quad O + H_2 \rightarrow OH + H$$

Colder peripheral region:

OH accumulation in HO_2 reactions

radial diffusion of H atoms;

$$H + O_2 + M \rightarrow HO_2 \quad ; \quad H + HO_2 \rightarrow OH + OH$$

[OH] kinetics in preheated fuel-air mixtures after ns pulse discharge burst

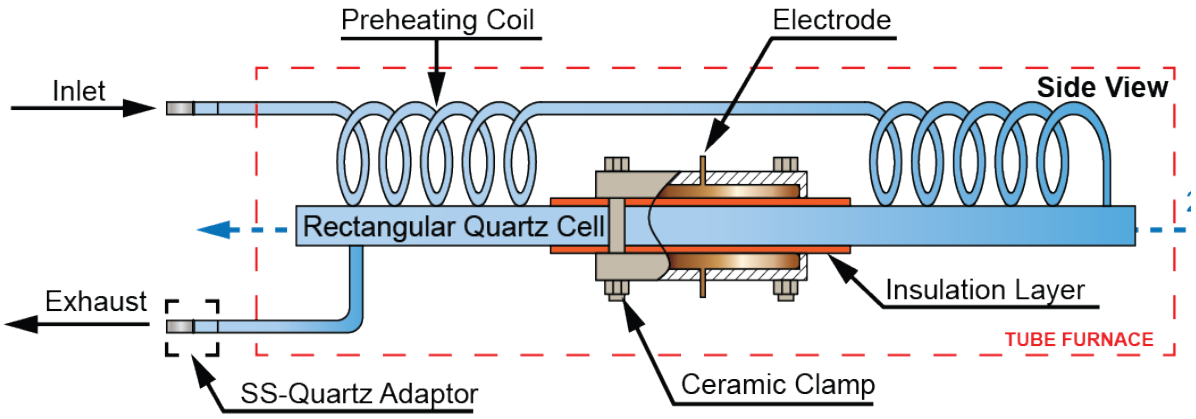

End View

	Pulse #10	Pulse #100
H_2 – air, ϕ=0.3 T_0=500 K, P=100 torr	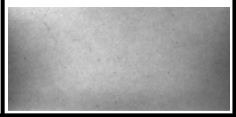	
C_2H_4 – air, ϕ=0.3 T_0=500 K, P=100 torr	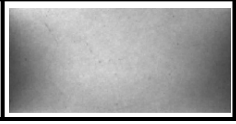	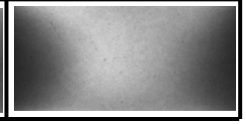

"Near 0-D" diffuse plasma, a burst of 50-100 pulses used to couple sufficient energy

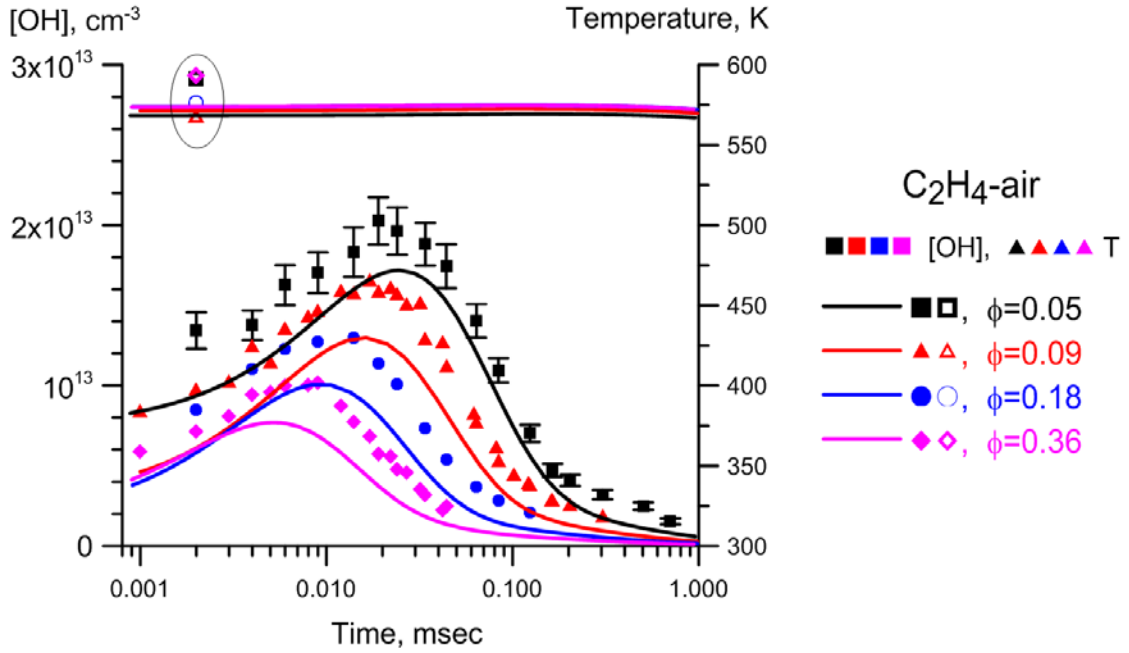

Comparison with modeling predictions: plasma assisted combustion kinetic mechanism validation

Plasma chemical reactions reduce ignition temperature in H_2-air

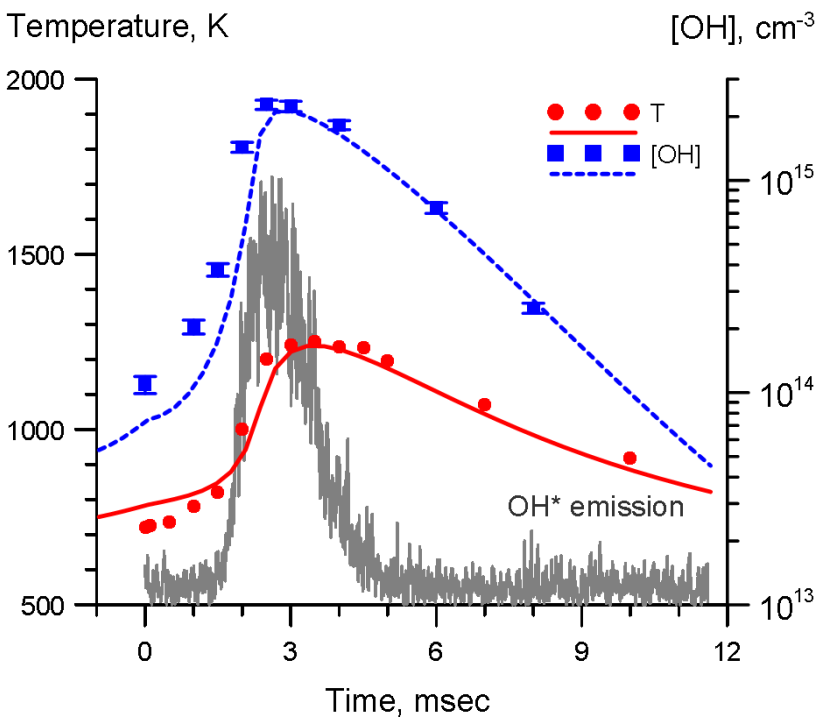

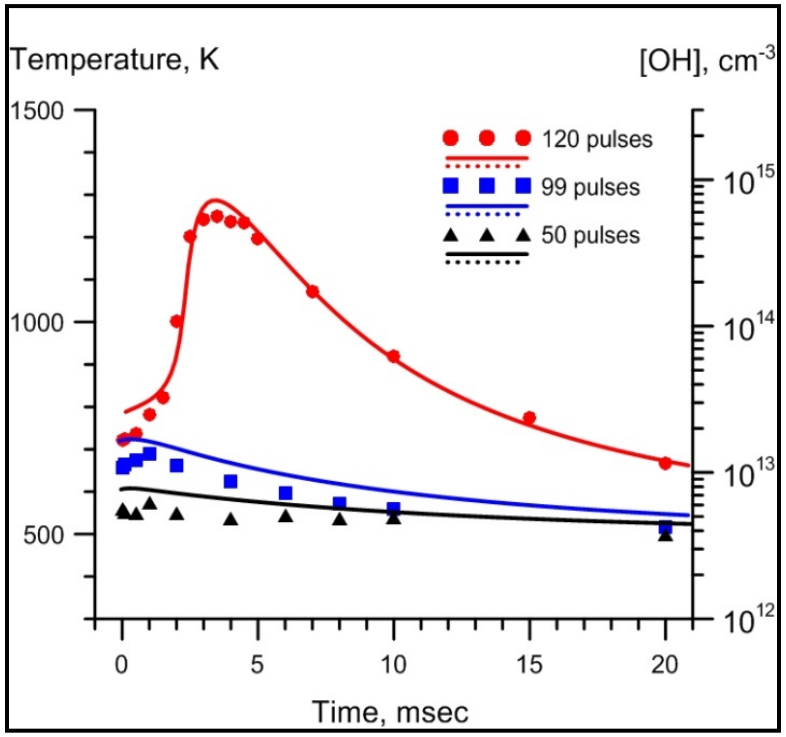

- ϕ=0.4, 120-pulse burst, T_0=500 K, P=80-90 torr
- Model predictions: good agreement with time-resolved temperature measurements
- Ignition temperature with plasma, $T_i \approx 700$ K, lower than autoignition temperature, $T_a \approx 900$ K

VI. Air plasma kinetics and plasma flow control

Ns DBD plasma actuators: subsonic flow boundary layer reattachment

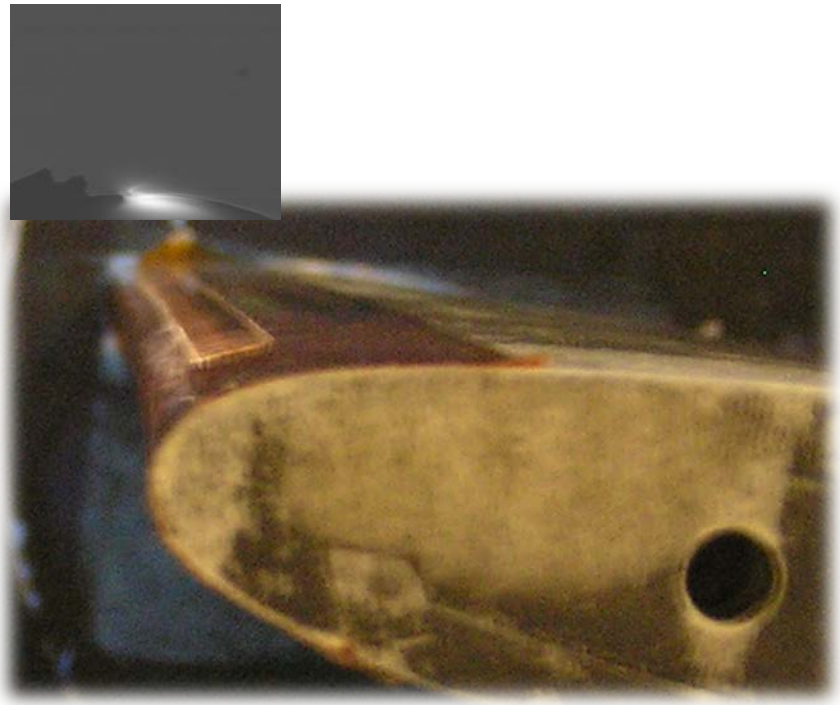

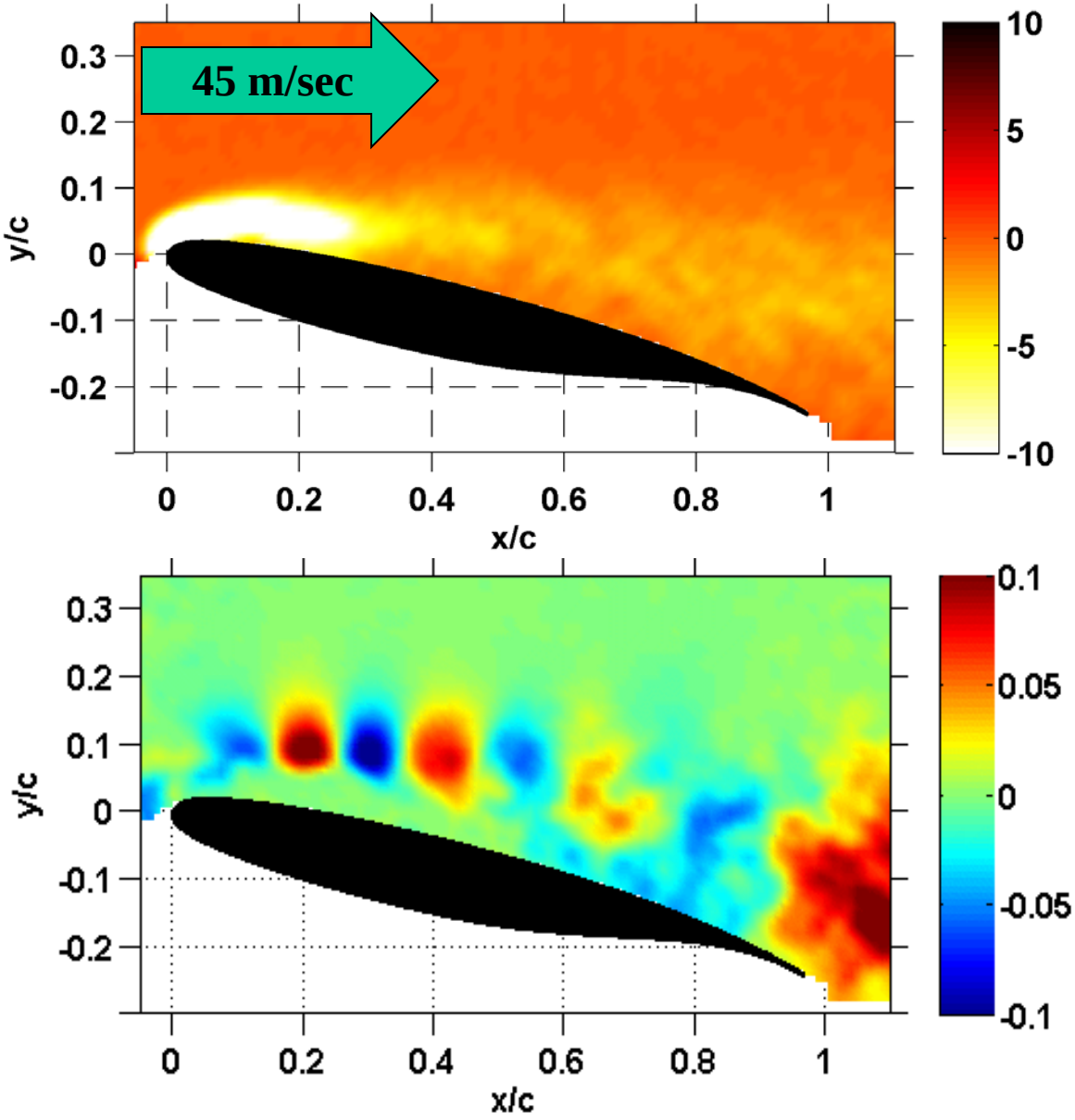

- Every nanosecond discharge pulse produces a robust spanwise vortex
- Enhanced mixing with free stream → boundary layer reattachment
- Same effect detected up to u=96 m/sec (M=0.28, Re_x~1.5 ·10^6)
- Consistently outperform AC DBD actuators

Localized Arc Plasma Flow Actuators (LAPFA):
Exciting instabilities in transonic and supersonic flows (M=0.9-2.0)

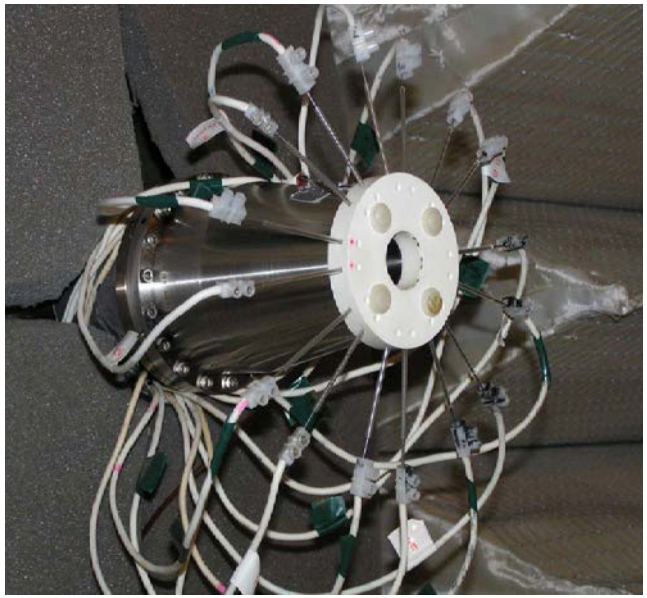

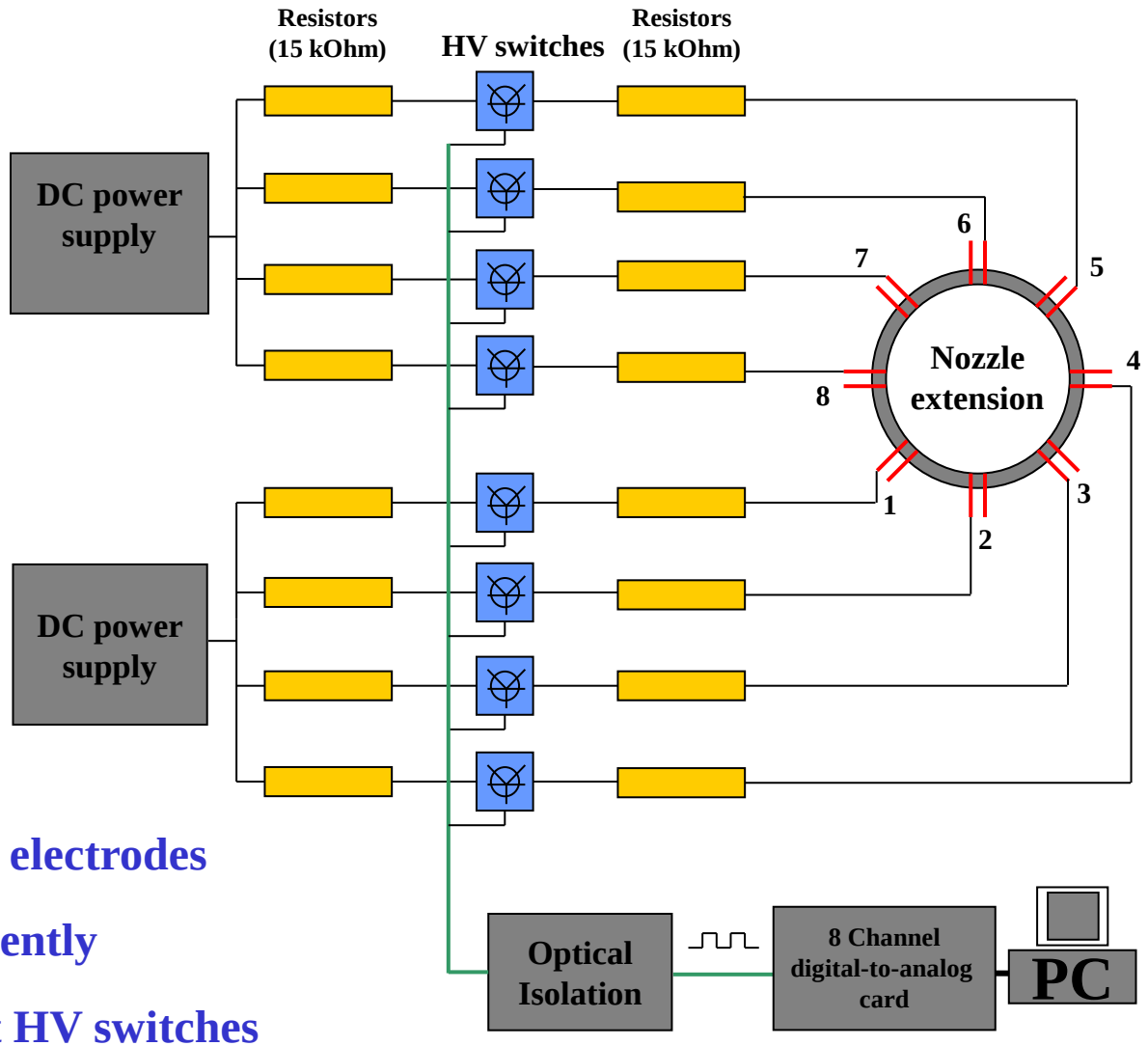

- BN nozzle extensions, tungsten wire electrodes
- Circular nozzle, 1 inch diameter recently
- Multiple channels controlled by fast HV switches
- Independent control of frequency, phase, and duty cycle → excitation of different instability modes

LAPFA: Formation of coherent structures in a M=0.9 circular jet

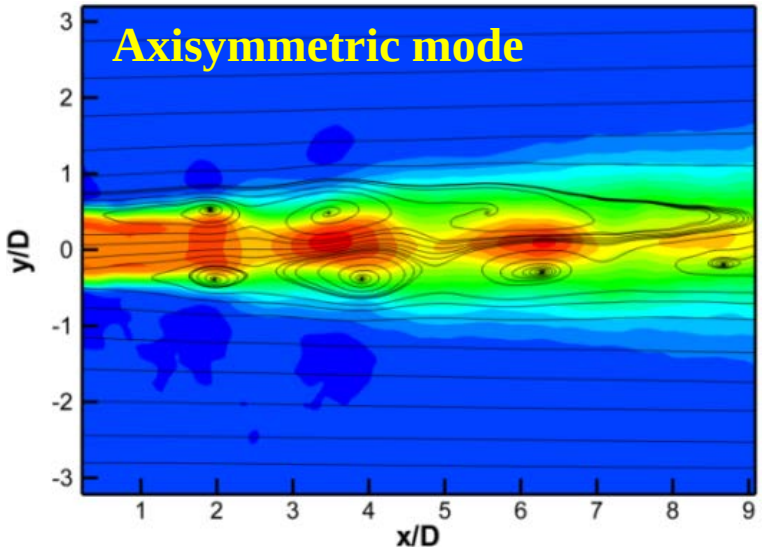

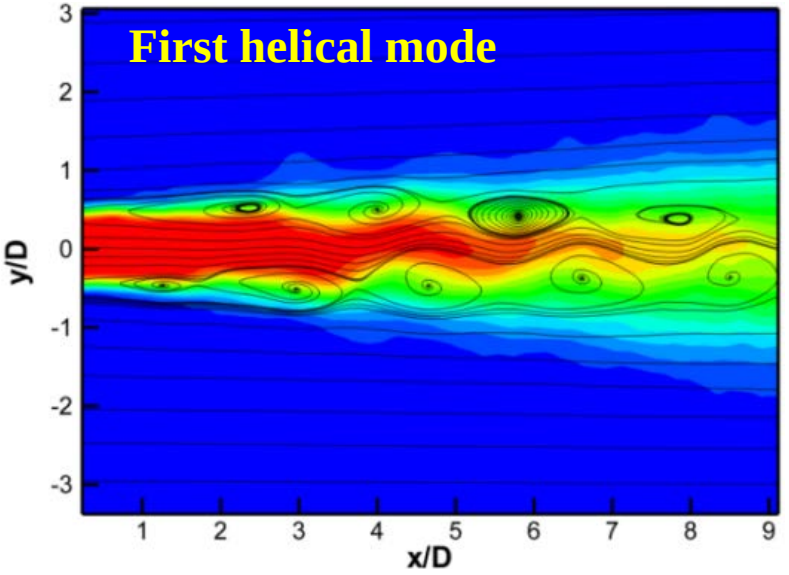

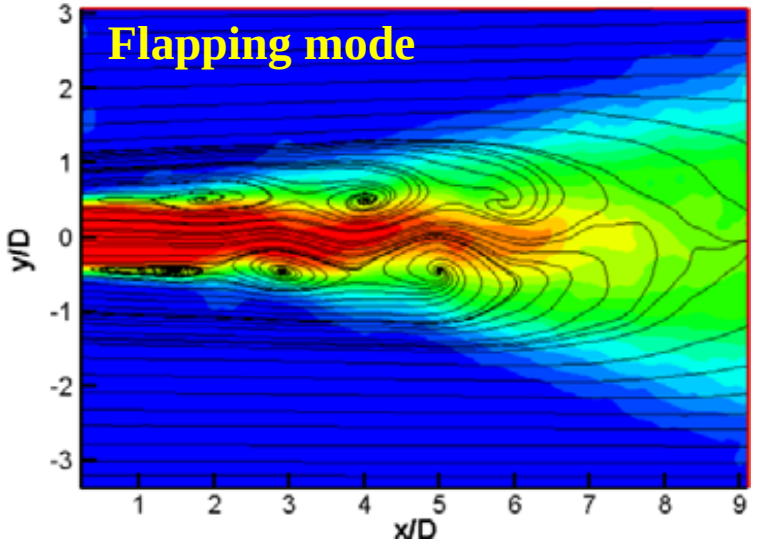

- High amplitude perturbations (localized heating in arc filaments)
- Every discharge pulse results in vortex formation
- Flow responds to forcing near jet column instability frequency

Control of supersonic mixing / shear layer by accelerated relaxation of vibrational energy

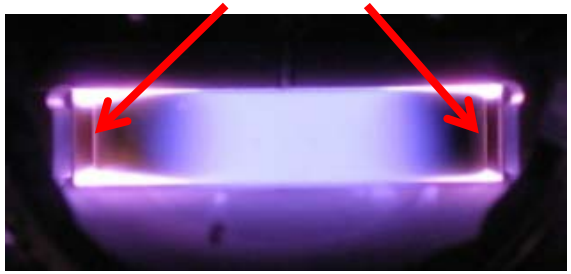

Flow into the page

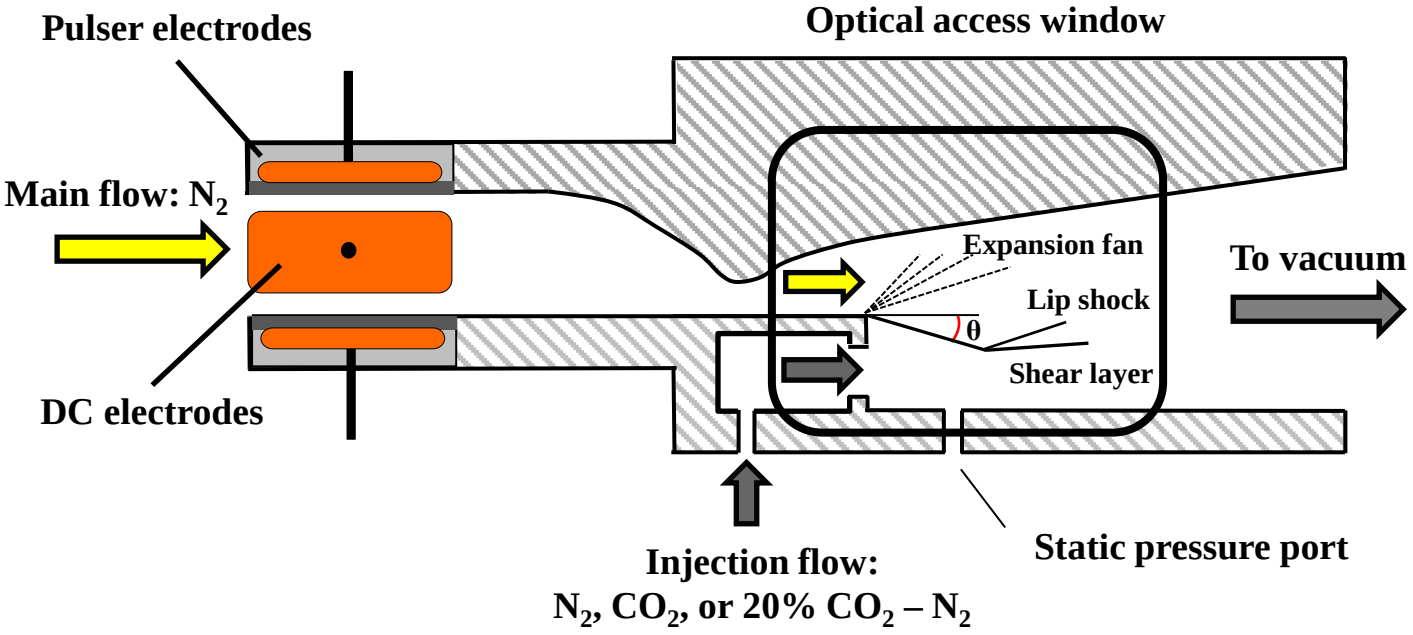

- Plenum: overlapped ns pulse / DC sustainer discharge for vibrational loading of N_2
- P_0 = 300 torr, T_V=2000, T=500 K, 2-D nozzle, top wall contoured, bottom wall plane
- Condition at nozzle exit : M = 2.5, P_{exit} = 15 torr
- Subsonic flow below expansion corner: injection of N_2 or CO_2
- Optical access for schlieren, CARS, and NO PLIF in subsonic and supersonic flows

Effect of vibrational relaxation of shear layer: N_2 / N_2 (left) vs. N_2 / CO_2 (right)

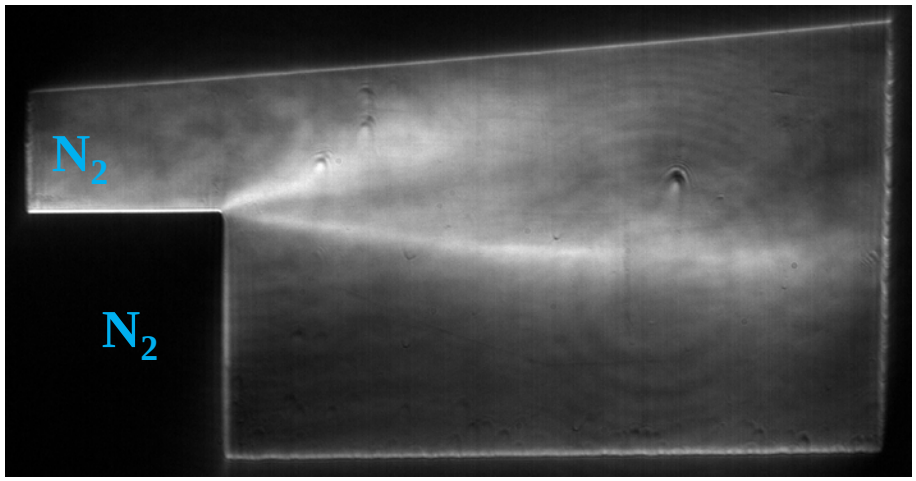

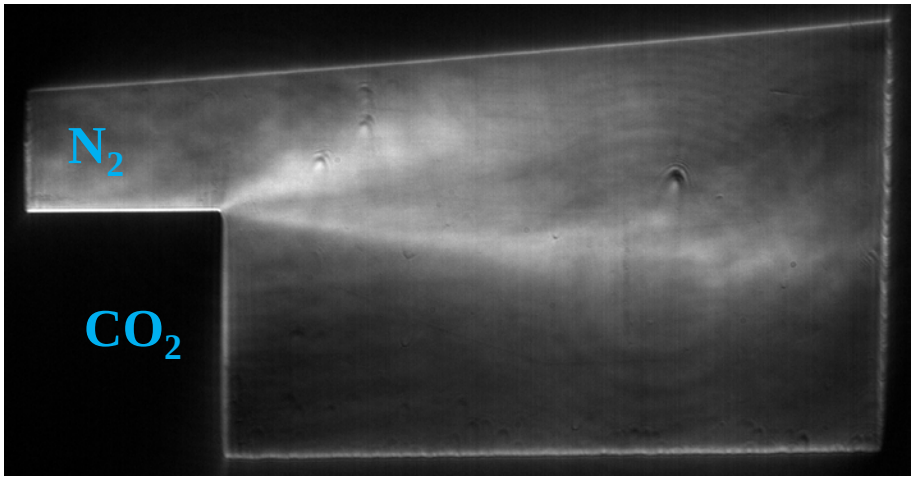

N_2 "bleeding" through backstep

CO_2 "bleeding" through backstep

- Time delay between frames 5 ms, t = 0-80 ms
- Ns pulse / DC discharge (2.3 kW) is turned on at t = 10-45 ms, to excite main N_2 flow
- No perturbation of shear layer detected in N_2 / N_2 flow
- In N_2 / CO_2 flow, shear layer expansion angle decreases, approaching $\theta=0^\circ$
- No change observed if main N_2 flow is not excited

N_2 Vibrational Temperature Distribution in Shear Layer

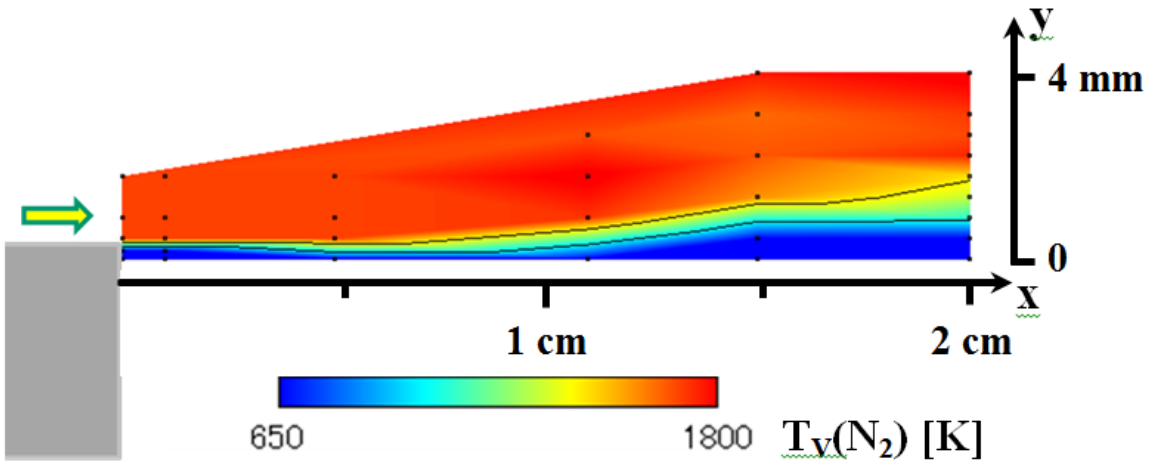

- Top flow: vibrationally excited N_2, T_V=1900 K, estimated T_{rot}=240 K
- Bottom flow: CO_2 bleeding through backstep, static pressure 7 torr

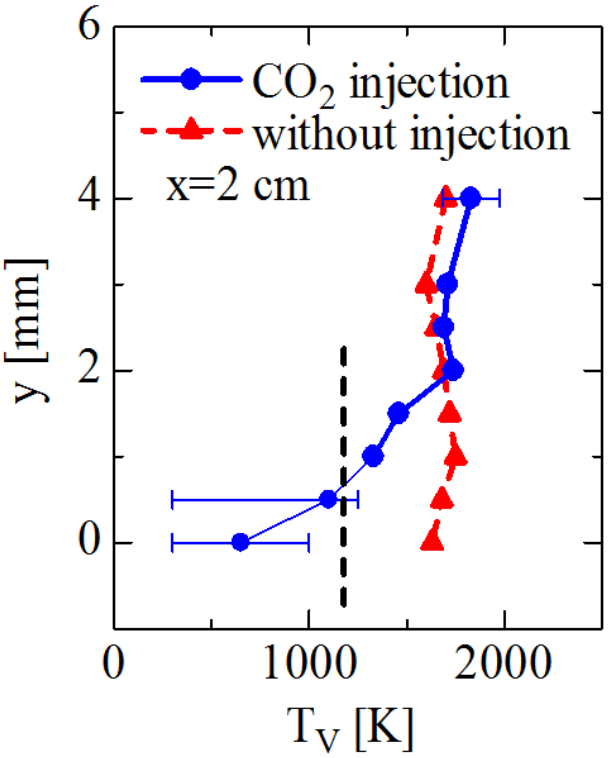

- CO_2 bleeding reduces $T_V(N_2)$, increases $T_{trans/rot}$ and static pressure
- Consistent with time-resolved measurements in ns pulse discharge in quiescent N_2-CO_2
- Static pressure increase pushes up shear / mixing layer

Summary: air plasma kinetics

- Growing body of time-resolved, spatially-resolved data characterizing transient, high-pressure air and fuel-air plasmas
- Measurements of electric field, electron density, and electron temperature necessary for insight into discharge energy coupling and partition
- Measurements of temperature, $N_2(v)$ populations, and excited electronic states of N_2^* necessary for insight into temperature dynamics
- Measurements of N_2^* and key radicals (O, H, OH, and NO) critical for quantifying their effect on fuel-air plasma chemistry
- Comparing measurement results with kinetic modeling predictions provides confidence in the models, assesses their predictive capability

Summary: nonequilibrium plasma flow control

- Surface and volumetric ns pulse discharges: energy thermalization on sub-acoustic time scale, high-amplitude compression wave generation
- Mechanism of energy thermalization ("rapid heating" and "slow heating") is well understood
- NS-DBD surface plasma actuators: large-scale coherent flow structures; significant flow control authority in subsonic flows (up to M = 0.3) at low actuator powers; scalable to large dimensions (~1 m)
- LAFPA actuators: large-scale coherent structures; excitation of flow instability modes; significant control authority in transonic and supersonic flows (M = 0.9-2.0) at low actuator powers; scalable to large phased arrays
- Flow control by vibrational relaxation: injection of "rapid relaxer" species into nonequilibrium flow at desired location; temperature and pressure rise due to accelerated relaxation; strong effect in supersonic shear layer

Acknowledgments

AFOSR MURI "Fundamental Mechanisms, Predictive Modeling, and Novel Aerospace Applications of Plasma Assisted Combustion"

AFOSR BRI "Nonequilibrium Molecular Energy Coupling and Conversion Mechanisms for Efficient Control of High-Speed Flow Fields"

DOE PSAAP-2 Center "Exascale Simulation of Plasma-Coupled Combustion" (under U. Illinois at Urbana-Champaign prime)

US DOE Plasma Science Center "Predictive Control of Plasma Kinetics: Multi-Phase and Bounded Systems"

NSF "Fundamental Studies of Accelerated Low Temperature Combustion Kinetics by Nonequilibrium Plasmas"